Size and dimensionality effects in superconducting Mo thin films

L Fàbrega[1], A Camón[2], I Fernández-Martínez[3], J Sesé[4], M Parra-Borderías[2], O Gil[1], R González-Arrabal[5], J L Costa-Krämer[3] and F Briones[3]

[1] Institut de Ciència de Materials de Barcelona (ICMAB-CSIC), Campus de la UAB, 08193 Bellaterra, Spain
[2] Instituto de Ciencia de Materiales de Aragón and Departamento de Física de la Materia Condensada, CSIC—Universidad de Zaragoza, E-50009, Zaragoza, Spain
[3] IMM—Instituto de Microelectrónica de Madrid (CNM-CSIC), Isaac Newton 8, PTM, E-28760 Tres Cantos, Madrid, Spain
[4] Instituto de Nanociencia de Aragón (Universidad de Zaragoza), C/Mariano Esquillor s/n, 50018 Zaragoza, Spain
[5] Instituto de Fusión Nuclear (Universidad Politécnica de Madrid), C/José Gutiérrez Abascal 2, 28006 Madrid, Spain

E-mail: lourdes@icmab.es (L Fàbrega)

Received 14 February 2011, in final form 13 May 2011
Published 1 June 2011
Online at stacks.iop.org/SUST/24/075014

Abstract
Molybdenum is a low T_c, type I superconductor whose fundamental properties are poorly known. Its importance as an essential constituent of new high performance radiation detectors, the so-called transition edge sensors (TESs) calls for better characterization of this superconductor, especially in thin film form. Here we report on a study of the basic superconducting features of Mo thin films as a function of their thickness. The resistivity is found to rise and the critical temperature decreases on decreasing film thickness, as expected. More relevant, the critical fields along and perpendicular to the film plane are markedly different, thickness dependent and much larger than the thermodynamic critical field of Mo bulk. These results are consistent with a picture of type II 2D superconducting films, and allow estimates of the fundamental superconducting lengths of Mo. The role of morphology in determining the 2D and type II character of the otherwise type I molybdenum is discussed. The possible consequences of this behaviour on the performance of radiation detectors are also addressed.

(Some figures in this article are in colour only in the electronic version)

1. Introduction

Transition edge sensors (TESs) are superconductor-based devices which work within the superconducting-to-normal transition, taking advantage of its sharpness. TES detectors are being developed for the detection of radiation across the electromagnetic spectrum from millimetres to gamma rays, as well as of weakly interacting particles and biomolecules. TES potential is now being realized in a variety of research fields, including particle physics, astronomy, biochemistry and materials science [1].

For TES fabrication, bilayers of normal/superconducting (N/S) films are preferred to single films. The transition temperature for the bilayer can be tuned by the proximity effect and their thermal diffusion can be enlarged by using noble metal layers with high residual resistivity ratios (RRR). Among the many N/S bilayers fabricated and tested [2–6], Mo-based bilayers have demonstrated to be one of the best choices. They have achieved the best spectral resolution in TES [6] and at present exhibit the best long-term stability.

The detectors performances are limited, among other factors, by the superconducting transition of the bilayer: its width, critical temperature and response to current and magnetic field. All of them are directly related to the electric and superconducting properties of the N and S layers. Hence, a deep understanding of the fundamental physics

that governs the superconducting-to-normal transition of these devices is essential for optimizing their design. However, even though superconductivity in Mo was discovered nearly 50 years ago [7], the superconducting properties of this metal have been poorly investigated. According to existing studies Mo has been shown to be a classical type I superconductor extremely sensitive to impurities [8, 9], weakly coupled, with critical temperature $T_c = 915$ mK and critical field $H_c = 98$ Oe [10–13]. Nevertheless, as far as we know, no experimental data on fundamental parameters such as penetration depth (λ) and coherence length (ξ) are available in literature. These parameters have only been estimated to be $\lambda \approx 96$ nm and $\xi \approx 271$ nm by French [14], from indirect calculations using other reported data for Mo bulk [10, 11, 15]; as the author states, the uncertainty in these estimates is high, and the reported values can be considered an upper and a lower limit of λ and ξ, respectively.

The T_c of a superconducting film is known to be influenced by its microstructure, in particular by the granular character [16–19] and by its thickness, for thin enough films [20–25]. Also, a transition 3D–2D character has been reported to occur when the film thickness becomes equal to the coherence length [26]. Since the disorder both enhances λ and reduces ξ [17], the granular character may affect the dimensional crossover and the onset of finite thickness effects. Moreover, for type I superconductors, as Mo is reported to be, a transition from type I to type II may occur. The changes in dimensionality and superconductivity type can result in significant modifications of the behaviour of the superconducting thin films under a magnetic field, since the critical fields can considerably change. Moreover, a 2D superconductor displays the Kosterlitz–Thouless transition [27], which demarks the spontaneous generation of vortex–antivortex pairs in zero field, due to fluctuations. All these effects generate sources of additional noise in devices such as TES detectors, and their systematic analysis may help to understand the performances of the TES and to improve reproducibility. In fact, it has been shown very recently that vortex motion is one of the fundamental processes responsible for excess noise in TES [28].

This work reports on a complete study of thickness and field effects in Mo thin films deposited at room temperature by magnetron sputtering. The deposition at room temperature, important for the mechanical stability of the detectors, implies a high degree of granularity, and therefore phenomena such as those just described may be quite relevant. The thickness dependences of resistivity, critical temperature and critical fields are used to analyse the superconducting character of the films and to provide new estimates for the fundamental superconducting lengths of Mo.

2. Experimental details

Mo thin films with thickness (d) ranging between 13 and 106 nm were deposited on top of Si single crystal substrates covered by a 300 nm Si_3N_4 layer, which will constitute the membrane in the future TES. The deposition was carried out by radio frequency (RF) magnetron sputtering, at room temperature and in an ultra-high vacuum (UHV) system with a base pressure of $\sim 10^{-8}$ Pa (10^{-10} mbar). The Ar working pressure was kept constant at 0.5 Pa (10^{-2} mbar) during sputtering and the RF power was fixed to 25 W. In most reported works high temperature deposition is required in order to obtain Mo films with good superconducting properties. We have demonstrated that they can also be obtained at room temperature, and this represents an advance for the development of Mo-based TES. Indeed, room temperature deposition minimizes the risk of interdiffusion (for instance, the formation of silicides is not expected to occur below 200 °C) and of thermal strains, and this improves the mechanical and chemical stability of the material and thus of the future device.

The films thickness was determined from x-ray reflectometry measurements. Structural and microstructural studies (texture, residual strain, grain size) were performed by x-ray diffraction and scanning electron microscopy, using respectively a Bruker D8 advance diffractometer with a GADDS two-dimensional detector and a QUANTA FEI 200 FEG-ESEM microscope. See Fàbrega *et al* [29] for further details on fabrication and structural characterization.

The film resistance was measured in a commercial physical property measurement system (PPMS) from Quantum Design Co., using the four-point resistance method and a current of 10 μA. Both $R(T)$ and $R(H)$ measurements were performed. The magnetic field was applied perpendicular and parallel to the films. For the latter orientation, the angular error was determined to be at most 0.25°. The T_c was defined as the middle point of the resistive transition (50% of the residual resistance value).

3. Results

3.1. Resistivity and critical temperature

Figure 1 displays the thickness dependence of the residual resistivity ρ_{res} and the superconducting critical temperature T_c for all measured films. It may be clearly seen that for the films thicker than ~30 nm both ρ_{res} and T_c are constant and similar to those reported earlier for 50 nm thick films deposited under the same conditions [29]. An enhancement of the resistivity and a reduction of T_c are observed for films thinner than ~25–30 nm. The room temperature resistivity (not shown) displays nearly the same dependence as ρ_{res}, indicating that ρ_{res} is the responsible of the observed variation in resistivity.

The measured changes in ρ_{res} and T_c might have several origins, such as stress, impurities and finite thickness effects. In order to elucidate them the possible contribution of the strain to the behaviour shown in figure 1 is first investigated. With this objective, the evolution of the lattice strain and that of the residual resistance ratio, RRR $= R(300\text{ K})/R(4.2\text{ K})$, with thickness are depicted in figure 2. Depending on d, three different strain regimes are observed: films thinner than ~25–30 nm present a rather high in-plane tensile strain, which relaxes when increasing d; films of ~50 nm are nearly relaxed (it is important to mention that the deposition conditions for these films were chosen to minimize the strain for 50 nm thick

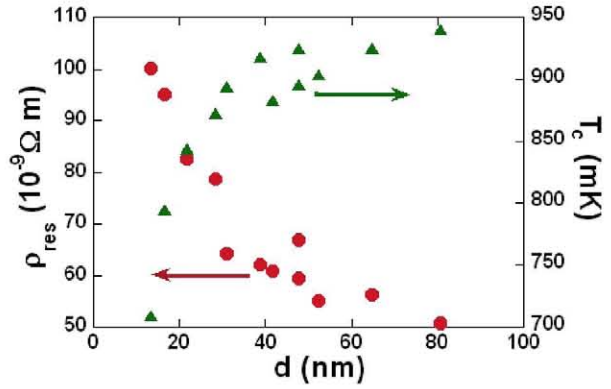

Figure 1. Thickness dependence of residual resistance $\rho_{res} = \rho$ (4.2 K) and superconducting critical temperature.

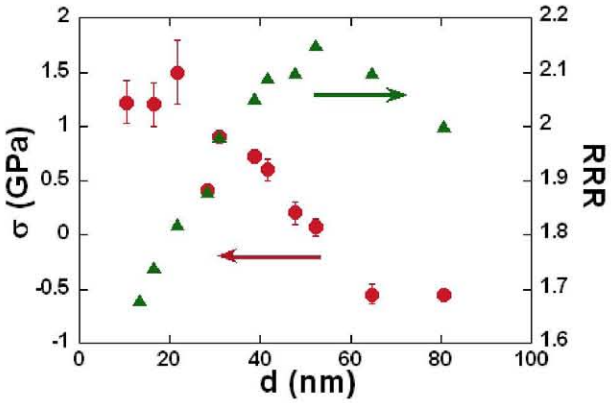

Figure 2. Thickness dependence of residual stress σ and residual resistance ratio.

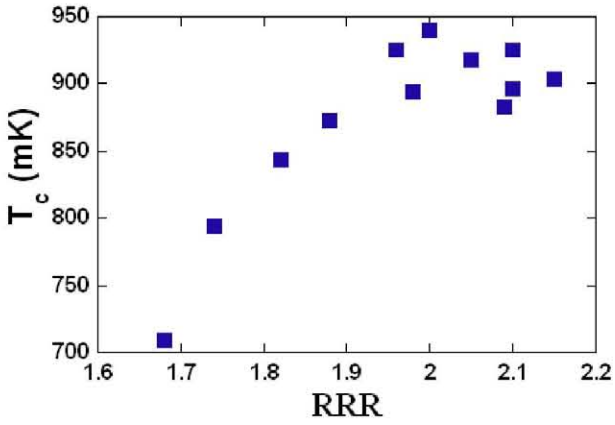

Figure 3. Critical temperature as a function of residual resistance ratio.

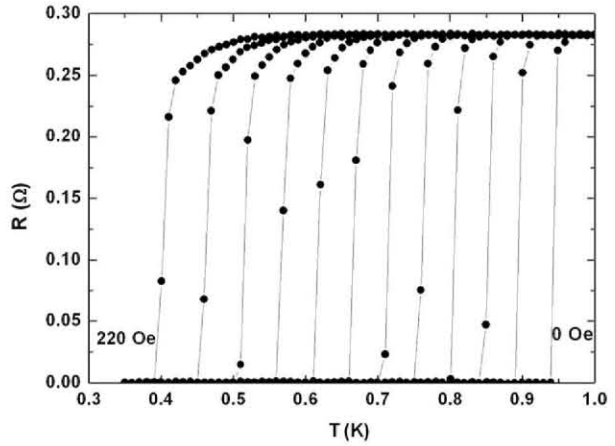

Figure 4. Resistive transitions under magnetic field applied perpendicular to the film with thickness 80.6 nm. The magnetic field was changed between 0 and 220 Oe with increments of 20 Oe.

films) [29], and films thicker than ~50 nm have a compressive in-plane strain. Concerning the RRR behaviour, it is seen that it monotonously increases with thickness for films thinner than ~50 nm, which is due to the decrease of ρ_{res} (figure 1). RRR shows a maximum for thickness values of ~50 nm and decreases for thicker films. This latter decrease reflects the previously reported dependence of ρ_{res} on compressive strain, which was ascribed to enhanced bulk scattering.

The dependence of T_c on RRR is shown in figure 3; T_c increases monotonously with RRR until its maximum value, and then saturates. This dependence is completely different from what is observed for films of constant thickness and different stress states, in which T_c (RRR) is a nearly linear decreasing function without a tendency to saturate [29].

All these results evidence that the observed changes in T_c and ρ_{res} for films thinner than ~50 nm have an origin completely different than those due to stress.

3.2. Critical field

In order to investigate the critical field and to find out if the films are type I or type II superconductors, their electrical and superconducting properties were investigated as a function of an external magnetic field, H, applied along the two main directions. The resistive superconducting transition for the 80.6 nm thick film, under several fields applied perpendicular to the film plane, is shown in figure 4. As expected, the transition shifts towards lower temperatures when increasing the magnitude of the external magnetic field. It is worth observing that superconductivity is still present in the film up to 370 mK for an applied field of 220 Oe. This is a significant result, since according to the literature the thermodynamic critical field of bulk Mo, which is known to be a type I superconductor, is much lower (~98 Oe) [8, 10–13].

Figure 5 displays the critical field values obtained for H applied perpendicular ($H^{\perp}$) and parallel ($H^{\parallel}$) to the film plane, as a function of $1/d$; the critical fields $H_c^{\perp}$ and $H_c^{\parallel}$ were determined from the middle point of the $R(H)$ transition recorded at 400 mK. The graph evidences that the critical field is highly anisotropic and thickness dependent, and that for both directions superconductivity persists up to fields much higher than the earlier reported thermodynamic critical field. Since the critical fields were measured at different reduced temperatures ($t = T/T_c$) because of the different T_c's of the films, the experimental values have been corrected using the conventional approximation for the Ginzburg–Landau temperature dependence of $H_c(T)$ and $\xi(T)$, $\sim(1 - t^2)$ and

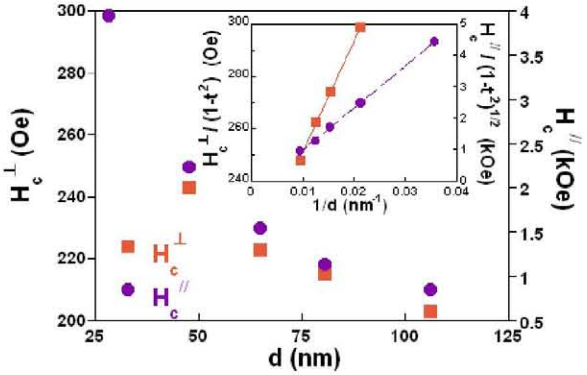

Figure 5. Critical fields measured parallel and perpendicular to the film plane. Inset: the same critical fields as a function of the reciprocal thickness. Note the different scales for both field orientations.

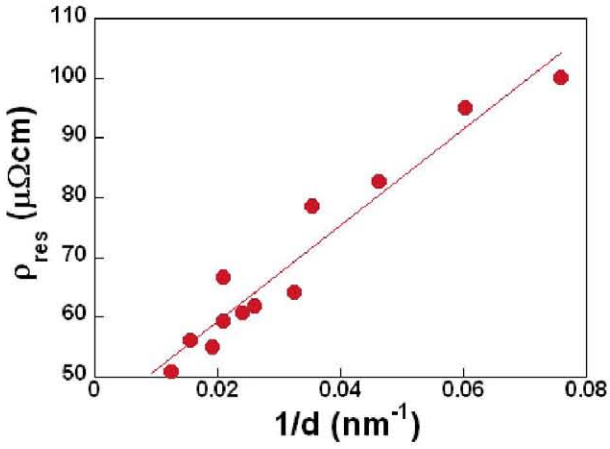

Figure 6. Residual resistivity as a function of reciprocal thickness.

$\sim(1 - t^2)^{-1/2}$ respectively (see equations (6) and (8) in section 4). The corrected data are depicted in the inset of figure 5. Both $H_c^{\perp}$ and $H_c^{\parallel}$ display a linear dependence on $1/d$, but with quite different slopes.

4. Discussion

4.1. Thickness dependence of ρ

A clear thickness dependence of both ρ_{res} and T_c is observed in figure 1 for films thinner than ~30 nm. This is the behaviour expected for size-effect samples i.e., for samples having some physical dimension comparable to the electron mean free path [30, 31]. As is known, the resistivity depends on size when the contribution to the resistivity arising from surface scattering of conduction electrons can no longer be ignored. For films in which the thickness dependence has been attributed to surface scattering, experimental data have been commonly analyzed on the basis of Fuchs theory [30]. For polycrystalline films, the enhancement of resistivity due to finite thickness follows the dependence [32]:

$$\rho = \rho_{\infty}(1 + A\ell_o/d). \tag{1}$$

Here A is a factor of the order of unity ($0 < A < 1$), ℓ_o is the electron mean free path, and ρ_{∞} is the resistivity of thick enough films; notice that this value may differ from that corresponding to the bulk metal, ρ_{bulk}, if the films are granular, because of the resistivity enhancement due to grain boundary scattering [31]. The dependence of ρ_{res} on the reciprocal thickness is shown in figure 6. As expected, these data clearly follow the behaviour predicted by equation (1). Moreover, from the linear fit $A\ell_o$ is estimated to be 19 nm, thus the mean free path value is very close to the column width of the films. This result points out that the resistivity in room temperature sputtered Mo films is dominated by grain boundary scattering, as argued by Fàbrega *et al* [29]. Consequently finite thickness effects in resistivity become relevant when the thickness is comparable to the grain size.

4.2. Thickness dependence of T_c

As shown in figure 1, T_c is strongly reduced for films thinner than ~30 nm. The T_c suppression due to finite thickness effects can be due to two mechanisms: (i) weak localization effects due to surface scattering [33], or (ii) the contribution to the superconducting free energy of the surface term, which becomes relevant for thin enough films [34]. In order to study which mechanism is the main one responsible for the T_c suppression observed in the measured films, the experimental data were interpreted in terms of both models.

The Maekawa and Fukuyama theory predicts that an enhanced Coulomb interaction between electrons produced by localization effects results in a reduction of T_c. In the frame of this theory the following relationship between the critical temperature and the sheet resistance R_{sheet} is established [33]:

$$\ln\left(\frac{T_c}{T_{co}}\right) = -\frac{g_1 N(0) e^2 R_{sheet}}{2\pi^2\hbar}\left[\frac{1}{2}\left[\ln\left(5.5\frac{\xi_o}{\ell_o}\frac{T_{co}}{T_c}\right)\right]^2 + \frac{1}{3}\left[\ln\left(5.5\frac{\xi_o}{\ell_o}\frac{T_{co}}{T_c}\right)\right]^3\right]. \tag{2}$$

T_{co} is the the bulk critical temperature, $g_1N(0)$ the effective coupling constant and ξ_o the BCS coherence length. If $\xi_o \gg \ell_o$, as in our case, the first term in the bracket becomes negligible, and a nearly linear dependence of T_c on R_{sheet} is expected [25, 35]. As shown in figure 7, the measured $T_c(R_{sheet})$ data can be fitted to this dependence but the slope obtained from the fit, when using $\xi_o = 271$ nm and $\ell_o = 20$ nm, provides an unrealistic $g_1N(0)$ value, two orders of magnitude larger than expected. Therefore, the weak localization effect cannot be considered to be the main responsible for the observed suppression of T_c at small d.

According to Simonin [34], the reduction of T_c due to the surface contribution to the free energy is described by the following dependence:

$$T_c = T_{co}\left[1 - \frac{2a}{N(0)V}\frac{1}{d}\right] \tag{3}$$

where a is the Thomas–Fermi screening length and $N(0)V$ is the bulk interaction potential. This expression allows

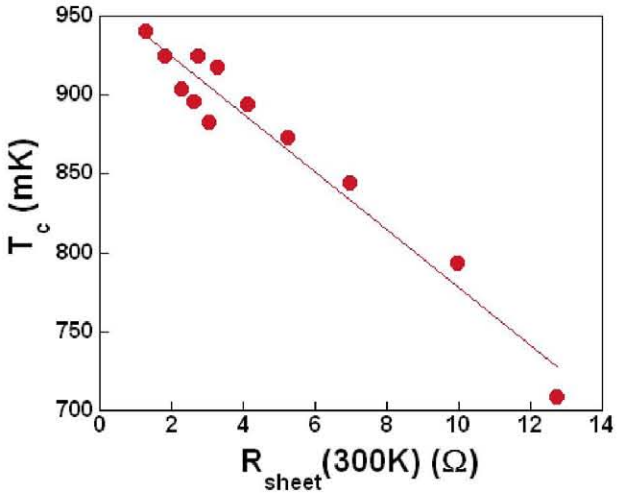

Figure 7. Critical temperature as a function of the sheet resistance.

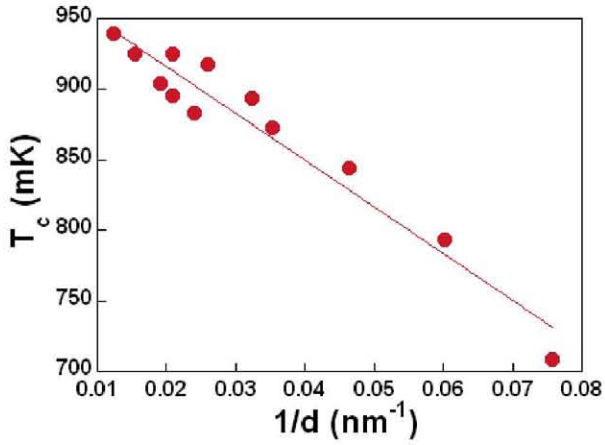

Figure 8. Critical temperature as a function of the reciprocal thickness.

us to define a critical thickness $d_m \equiv 2a/N_o V$ at which superconductivity disappears.

The T_c as a function of the reciprocal thickness for all characterized films is depicted in figure 8. A nearly linear dependence of T_c on $1/d$ is observed. From the data fit, making use of $N_o V = 0.157$ for Mo [13], the Thomas–Fermi screening length is calculated to be 0.3 nm. This value is in excellent agreement with a theoretical estimation using the value of the Fermi length for Mo reported by Boucher *et al* [36], $\lambda_F = 0.365$ nm. Even more, the critical thickness at which T_c becomes zero turns out to be $d_m \sim 4$ nm. Thus, all presented data support that the reduction of the order parameter near the superconductor surfaces [34] seems to be the main responsible mechanism of the T_c suppression mechanism due to finite thickness, for the studied films.

4.3. Critical fields

As is well known the superconductor type depends on the ratio between the penetration depth and the coherence length, $\kappa \equiv \lambda/\xi$. Moreover, the superconducting purity may affect these characteristic lengths. Since for the analyzed films ℓ_o has been estimated to be ~20 nm, and the lower limit of the Mo coherence length has been reported to be $\xi_o \sim 271$ nm [14], one can conclude that these Mo films are in the dirty limit ($\ell_o \ll \xi_o$). For dirty superconductors, the fundamental superconducting lengths must be renormalized according to the following expressions [37]:

$$\xi(0) \approx 0.85\sqrt{\xi_o \ell_{eff}} \qquad \lambda_{GL}(0) \approx \lambda_L(0)\left(\frac{\xi_o}{1.33\ell_{eff}}\right)^{1/2} \quad (4)$$

where $\xi(0)$, $\lambda_{GL}(0)$ and $\lambda_L(0)$ are the zero temperature Ginzburg–Landau coherence length, the penetration depth and the London penetration depth respectively, and ℓ_{eff} is the effective mean free path. These equations evidence that for a dirty superconductor the coherence length and the penetration depth are correspondingly directly and inversely proportional to $\ell_{eff}^{1/2}$. Thus, an enhancement in the κ parameter value is expected when reducing the mean free path according to:

$$\kappa \approx 0.74\lambda_L(0)/\ell_{eff}. \quad (5)$$

By inserting in equation (5) the λ_L value reported for Mo ($\lambda_L(0) = 96$ nm) [14], which was argued to correspond to an upper limit, we obtain that when ℓ_{eff} is lower than ~140 nm Mo should behave as a type II superconductor. Therefore, all characterized films are expected to behave as type II superconductors, and consequently the critical field obtained from the $R(T, H)$ data should correspond to the upper critical field H_{c2}, which for a film in the perpendicular orientation can be written as [38]

$$H_{c2}^{\perp}(T) = \sqrt{2}H_c(T)\kappa \approx H_c(T)\lambda_L(0)/\ell_{eff}. \quad (6)$$

Here $H_c(T)$ is the thermodynamic critical field of the superconductor. As shown by equation (1) and in [30] the effective mean free path ℓ_{eff} is thickness dependent and can be approximated to

$$1/\ell_{eff}(d) = 1/\ell_o + A/d \quad (7)$$

where ℓ_o is the mean free path of an infinitely thick film.

Equations (6) and (7) reveal that $H_{c2}^{\perp}$ follows a $1/d$ law, as observed in the inset in figure 5. By linearly fitting these data an estimation of $A\ell_o \sim 21$ nm is obtained, in excellent agreement with that previously found from the $\rho(d)$ dependence. Also, by assuming $H_c \approx 98$ Oe [8, 10–13], the fit provides an estimate of 44 nm for $A\lambda_L(0)$, somehow smaller than the value derived by French [14], which was in fact considered an upper limit for the penetration depth, as argued in section 1.

We focus now on the upper critical field parallel to the film. Considering the earlier reported lower limit for the coherence length value of Mo, $\xi_o \approx 271$ nm [14], equations (4) indicate that for the studied thickness range it is likely that $\xi(T) > d$, which points out that the analyzed films might be 2D superconductors. The parallel upper critical field for a 2D superconductor is defined by [26]:

$$H_{c2}^{\parallel}(T) = \frac{\sqrt{12}\phi_o}{2\pi\mu_o\xi(T)d}. \quad (8)$$

As shown in the inset of figure 5 $H_c^{\parallel}$ follows a $1/d$ dependence, in agreement with that predicted in equation (8). The corresponding linear fit provides $\xi(0) \approx 85$ nm. Inserting this value in equation (4), and using[6] $\ell_{eff} \approx \ell_o \approx 20$ nm an estimate for $\xi_o \approx 500$ nm is obtained. This value is larger than the reported $\xi_o \approx 271$ nm, which was argued to correspond to a lower limit [14], and corroborates the assumed 2D character of the Mo films.

The fact that the studied films are 2D superconductors is an important issue for Mo-based high performance radiation detectors. It might have relevant implications in view of sensor development; indeed, for instance, the thermal fluctuations of the order parameter in a 2D superconductor can lead to a Kosterlitz–Thouless transition [27], associated with the spontaneous creation of vortex–antivortex pairs. These fluctuations may constitute a significant noise source [28] and thus would deserve further study. Also, it is worth noting that the fundamental lengths of Mo are strongly affected by the grain size of the films, and thus by the fabrication conditions, which determine the films' microstructure. For highly disordered films, this implies that transitions from type I to type II superconductor and from 2D to 3D behaviour might occur for Mo films with thicknesses close to those usually employed in proximity bilayers for TES ($d \sim 50$ nm); furthermore, the effective coherence length determines the maximum d to observe the proximity effect [1]. Therefore, accurate estimates of the coherence length of Mo—both for bulk Mo and for thin films—, as well as further studies of the possible 2D character of the films and its effects on the behaviour under magnetic field and on noise will be quite important to tailor the detectors.

5. Conclusions

Summarizing, Mo thin films deposited by sputtering at room temperature are highly disordered, with a resistivity dominated by grain boundary scattering, so that the electronic mean free path is limited to the lateral grain size, $D \sim 20$ nm. As a consequence, the films display finite thickness effects both in the normal state resistivity and in the superconducting critical temperature when d approaches this characteristic length. The resistivity enhancement at small thicknesses has been shown to be mainly due the contribution of surface scattering, while the reduction of the critical temperature may be principally ascribed to the reduction of the order parameter near the superconducting surfaces.

The critical magnetic field has been found to be anisotropic, thickness dependent and larger than that reported for Mo bulk. This behaviour is consistent with a picture of a dirty superconductor, in which the lateral grain size limits the mean free path and modifies the superconducting fundamental lengths accordingly, so that the films behave as 2D type II superconductors. These observations illustrate that for granular films the superconducting fundamental lengths can be sensibly altered, and therefore modify the type and dimensionality of the superconductor; furthermore, type and dimensionality crossovers can take place right within the thickness ranges used for applications as TES detectors. These findings are extremely relevant for further development of Mo-based high sensitivity detectors in order to be able to predict and estimate possible noise sources, magnetic field sensitivity, current carrying capabilities and/or difficulties in their performance.

Finally, the fundamental lengths for Mo have been estimated. These data allow the determination of the Mo superconducting thin films' properties which, as far as we know, has not been previously done due to the scarcity of experimental data on this superconductor.

[6] An accurate estimate would require introducing equation (7) in the expression of $\xi(0)$ in equation (4) and using it for the fit to equation (8); however, and in opposition to what happens for the perpendicular field direction, the effect of the thickness dependence of $\ell_{eff}(d)$ is quite small, because in equation (8) the $1/d$ factor dominates, while in equation (6) the d dependence of $\ell_{eff}(d)$ is only responsible for the thickness dependence of the perpendicular critical field.

Acknowledgments

This work has been supported by the Spanish Ministerio de Ciencia e Innovación, MCINN (projects ESP2006-13608-C02, AYA2008-00591/ESP, MAT2008-01077/NAN and MAT2009-13977-C03). OG and MPB thank MCINN for their fellowships.

References

[1] Irwin K D and Hilton G C 2005 *Cryogenic Particle Detection* (*Topics in Applied Physics* vol 99) ed C Enss (Berlin: Springer) pp 63–149 and references therein
[2] Irwin K D, Hilton G C, Wollman D A and Martinis J M 1996 *Appl. Phys. Lett.* **69** 1945
[3] Hohne J *et al* 1999 *X-ray Spectrom.* **28** 396
[4] Dirks B P F *et al* 2009 *Nucl. Instrum. Methods* A **610** 83
[5] Tan P *et al* 2002 *AIP Conf. Proc.* **605** 255
Rajteri M, Monticone E, Gandini C, Portesi C, Rocci R and Bodoardo S 2003 *IEEE Trans. Appl. Supercond.* **13** 3292
[6] Bandler S R *et al* 2008 *J. Low Temp. Phys.* **151** 400
Iyomoto N *et al* 2008 *Appl. Phys. Lett.* **92** 013508
[7] Geballe T H, Matthias B T, Corenzwit E and Hull G W Jr 1962 *Phys. Rev. Lett.* **8** 313
[8] Yakov D' and Svets A D 1966 *Sov. Phys.—JETP* **22** 759
[9] Schmidt P H, Castellano R N, Barz H, Cooper A S and Spencer E G 1976 *J. Appl. Phys.* **44** 1833
Linker G and Meyer O 1976 *Solid State Commun.* **20** 695
[10] Hein R A, Gibson J W, Pablo M R and Blaugher R D 1963 *Phys. Rev.* **129** 136
[11] Rorer C, Onn D G and Meyer H 1965 *Phys. Rev.* **138** A1661
[12] Waleh A and Zebouni N H 1971 *Phys. Rev.* B **4** 2977
[13] Mallon R G and Rorschach H E 1967 *Phys. Rev.* **158** 418
[14] French R A 1967 *Phys. Status Solidi* **21** K35
[15] Fawcett E and Griffiths D 1962 *J. Phys. Chem. Solids* **23** 1631
[16] Crow J E, Strongin M, Thompson R S and Kammerer O F 1969 *Phys. Lett.* A **30** 161
[17] Hauser J J and Theuerer H C 1964 *Phys. Rev.* **134** A198
Abeles B, Cohen R W and Stowell W R 1967 *Phys. Rev. Lett.* **18** 902
Bose S, Raychaudhuri P, Banerjee R and Ayyub P 2006 *Phys. Rev.* B **74** 224502
[18] Deutscher G, Entin-Wohlman O and Shapira Y 1980 *Phys. Rev.* B **22** 4264
[19] Gubin A I, Il'in K S, Vitusevich S A, Siegel M and Klein N 2005 *Phys. Rev.* B **72** 064503
[20] Wolf S A, Kennedy J J and Nisenoff M 1976 *J. Vac. Sci. Technol.* **13** 145
[21] Park S I and Geballe T H 1985 *Physica* B **135** 108
Quaterman J H 1986 *Phys. Rev.* B **34** 1948

[22] Oshima K, Kuroishi T and Fujita T 1976 *J. Phys. Soc. Japan* **41** 1234
[23] Jiang Q D *et al* 1990 *J. Phys.: Condens. Matter* **2** 3567
[24] Ilin K S *et al* 2004 *Physica* C **408–410** 700
[25] Minhaj M S M, Meepagala S, Chen J T and Wenger L E 1994 *Phys. Rev.* B **49** 15235
[26] See for instance Jin B Y and Ketterson J B 1989 *Adv. Phys.* **38** 189
[27] Kosterlitz J M and Thouless D J 1983 *J. Phys. C: Solid State Phys.* **6** 1181
Minnhagen P 1987 *Rev. Mod. Phys.* **59** 1001
[28] Galeazzi M 2010 *Proc. ASC, IEEE Trans. Appl. Supercond.* doi:10.1109/TASC.2010.2091243
[29] Fàbrega L *et al* 2009 *IEEE Trans. Appl. Supercond.* **19** 3779
[30] See e.g. Sondheimer E H 1952 *Adv. Phys.* **1** 1
[31] Coutts T J 1974 *Electral Conduction in Thin Metal Films* (Amsterdam: Elsevier)
[32] Mayadas A F and Shatzkes M 1970 *Phys. Rev.* B **1** 1382
[33] Maekawa S and Fukuyama H 1981 *J. Phys. Soc. Japan* **51** 1380
[34] Simonin J 1986 *Phys. Rev.* B **33** 7830
[35] Graybeal J M and Beasley M R 1984 *Phys. Rev.* B **29** 4167
[36] Boucher R *et al* 2006 *Supercond. Sci. Technol.* **19** 138
[37] Tinkham M 1996 *Introduction to Superconductivity* (Singapore: McGraw-Hill) pp 118–20
[38] Tinkham M 1996 *Introduction to Superconductivity* (Singapore: McGraw-Hill) p 135